Journal Pre-proof

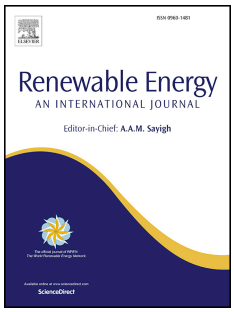

Optimization of FAME production from blends of waste cooking oil and refined palm oil using biomass fly ash as a catalyst

Edgar M. Vargas, Lizeth Ospina, Márcia C. Neves, Luís A.C. Tarelho, Maria I. Nunes

PII: S0960-1481(20)31596-2

DOI: https://doi.org/10.1016/j.renene.2020.10.030

Reference: RENE 14320

To appear in: *Renewable Energy*

Received Date: 19 December 2019

Revised Date: 11 September 2020

Accepted Date: 6 October 2020

Please cite this article as: Vargas EM, Ospina L, Neves MáC, Tarelho LuíAC, Nunes MI, Optimization of FAME production from blends of waste cooking oil and refined palm oil using biomass fly ash as a catalyst, *Renewable Energy* (2020), doi: https://doi.org/10.1016/j.renene.2020.10.030.

Credit author statement

Edgar M. Vargas: Conceptualization, Methodology, Investigation, Validation, Formal Analysis, Resources, Writing-Original draft preparation

Lizeth Ospina: Investigation

Márcia C. Neves: Investigation

Luís A. C. Tarelho: Resources

Maria I. Nunes: Conceptualization, Methodology, Writing-Reviewing and Editing, Supervision

Optimization of FAME production from blends of waste cooking oil and refined palm oil using biomass fly ash as a catalyst

Edgar M. Vargas[a,c], Lizeth Ospina[a], Márcia C. Neves[b], Luís A. C. Tarelho[c], Maria I. Nunes[c,*]

[a] Dep. of Chemical Engineering, University Jorge Tadeo Lozano, Bogotá, Colombia

[b] Dep. of Chemistry and CICECO, University of Aveiro, Portugal

[c] Centre for Environmental and Marine Studies, Dep. of Environment and Planning, University of Aveiro, Portugal

Abstract

One of the problems associated with biomass combustion is the amount of fly ashes generated and its subsequent management. The search for ways of valorizing these ashes has been a challenge for the academic and industrial community. On the other hand, used cooking oils are wastes which management is quite difficult, by they have a very important energetic potential. The goal of this work was to optimize the Fatty Acid Methyl Esters (FAME) process, recovering two residual materials (waste cooking oils (WCO), and biomass fly flash (BFA)). The optimization of the process was achieved using the response surface methodology and a Box-Benhken experimental design applied to mixtures of WCO and refined palm oil (RPO), using BFA as catalyst. The influence on FAME yield of four variables (catalyst loading, methanol/oil molar ratio, RPO/WCO ratio and reaction

* Corresponding author. Tel.: +351 234 370 349

E-mail address: isanunes@ua.pt; isanune@gmail.com (M.I. Nunes)

Postal Code: 3810 – 193 Aveiro, Portugal.

temperature) was studied. The higher FAME yield achieved was 73.8 % for the following operating conditions: 13.57 wt% of catalyst loading, 6.7 of methanol/oil molar ratio, 28.04 wt% of RPO in the oil mixture with WCO and 55^{o}C for the reaction temperature. The reusability of the BFA catalyst in the process was also studied through three successive usage cycles finding no loss of catalytic activity.

Keywords: Biomass fly ash; FAME; optimization; refined palm oil; response surface methodology; waste cooking oil.

1 Introduction

The production of biodiesel has become a very important area of research due to the rapid depletion of energy reserves and the increase in oil prices along with environmental concerns [1]. In the current situation, the foremost amount of energy is supplied by the conventional fossil fuel resources, such as gasoline, liquefied petroleum gas, diesel fuel, coal and natural gas. It is imperative to find alternative fuels to the petroleum based ones in order to, along with environmental issues, prolong the petroleum supply. One of the most promising biofuel is biodiesel, a “green fuel” alternative to diesel fuel, derivate from renewable sources with high quality [2]. The integration of wastes as a catalyst or as an (vegetable) oil feedstock into the biodiesel production process can be a promising way to reduce environmental burdens and the production costs, while also aligning with the principles of circular economy.

Globally, the cost of production has been the main barrier in commercializing biodiesel. In the literature, it is consensual that the oily feedstock is the major contributor, about 80 %

[3], for the total production costs. The waste cooking oils (WCO) are edible vegetable oils that have been previously used for frying or cooking and can constitute an additional source of raw material for biodiesel production. This feedstock can be two to three times cheaper that virgin vegetable oils [4,5]. Furthermore, it is generally accepted that reusing WCO for human consumption is harmful to health and this waste is difficult to manage [6].

It is important to mention that the catalyst commonly used in the biodiesel production is the sodium or potassium hydroxide, which have been economically unfeasible to recover from the process. Aiming to tackle this hotspot of the process, some research [7–9] have been focused on the exploitation of waste materials (e.g. shells, ashes, peels and bones), due to their abundance and low cost, for solid catalysts preparation. On the other hand, biomass fly ashes (BFA) are a residual materials whose disposal and management represent a significant challenge [10], given its increasing production over the last two decades [11]. The development of alternative solutions for BFA proper utilization/valorization with emphasis on finding new applications is currently a very important issue [12]. The use of BFA, as a (heterogeneous) catalyst, on the biodiesel production process has been proving to be a promising alternative to valorize this waste; it has been found that BFA have a potential for catalyzing the reactions for FAME (Fatty Acid Methyl Esters) production and have bifunctional characteristics (acid and basic) that allow catalyzing transesterification and esterification reactions simultaneously [13].

The main objective of this work was to optimize the FAME production process using mixtures of WCO and refined palm oil, and BFA as catalyst. The effect on FAME yield of four operating variables was tested, namely: catalyst loading, methanol/oil molar ratio,

RPO/WCO mass ratio and reaction temperature. Additionally, it was carried out a study of reusability of the catalyst aiming to assess its performance over several cycles of utilization in the FAME synthesis process.

2 Material and Methods

The Box-Benhken experimental design and Response Surface Methodology (RSM) were used to design the experiments to optimize the FAME production process and for the data treatment.

Previously, the solid catalyst (BFA) was prepared and characterized in terms of some of its chemical, physical and structural properties. The raw-material for FAME synthesis consisted of a blends of WCO and RPO in different ratios. The adopted procedures are described in the next sections as well as the analytical methods used.

2.1 Materials

Waste cooking oil for FAME production was provided by a local collecting company (Bioils) in Bogotá, Colombia. The WCO was pre-treated by filtration to remove suspended particles and heating (at 110 °C for 1 h) to eliminate traces of water. The RPO was purchased at a local store in Bogotá. The BFA came from a dedusting system (electrostatic precipitator) of a thermal power-plant using residual forest biomass (mainly derived from eucalyptus) sited in the Centre Region of Portugal.

All the chemicals used were analytical grade except n-hexane (GC grade) and methyl heptadecanoate (analytical standard) from Sigma-Aldrich and Merck.

2.2 Oil mixtures characterization

According to the experimental design presented in Section 2.5, three oily feedstock were prepared using different mass ratios of RPO/WCO: M1 (100 % RPO), M2 (50 % RPO, 50 % WCO) and M3 (0 % RPO). These mixtures were characterized in terms of: acid value (NTC 218) [14], density (NTC 336) [15], saponification number (NTC 335) [16], viscosity (ASTM D445 and ASTM D446) [17,18], and moisture content (Karl Fisher, Coulometer 831-Metrohm).

The saponification number (*SN*) was used to calculate the molecular mass (*MW*, g/mol) according to Eq. 1 [3].

$$MW = \frac{56.1 \times 1000 \times 3}{SN} \quad (1)$$

The FFA content was calculated from the acid value (*AV*, mg KOH/g) using Eq. 2 [3].

$$\text{FFA} = \frac{AV}{2} \quad (2)$$

2.3 Catalyst preparation and characterization

Usually the solid catalysts are characterized by different instrumental techniques in order to measure their morphology, physical properties and bulk properties. The catalytic behavior depends on the morphological characteristics of the solid material, because the catalytic

process takes place at its surface (outer and inner). The most utilized techniques to characterize materials' morphology are BET and SEM. In terms of physical properties, the surface area is the place of catalytic activity, but only a part is utilized in the catalytic reaction (active center). In basic and acid catalysts, the active sites not only occupy a little fraction of the surface, but also differ in basic and acid strength and sometimes in nature. Hammett indicators are often used to determine the acid and basic strengths of a material. FTIR is useful to identify the main chemical functional groups present on the surface of solid materials. For bulk properties X-ray diffraction (XRD) is used to find: (i) the crystalline phases, (ii) crystalline degree and (iii) crystallite size [19], with which the catalytic activity can be interpreted.

In this work, the catalyst was prepared by drying the fly ash (BFA) for 2 hours at 120 ^{o}C. Then, the resulting material was characterized in terms of: (i) crystallographic structures, by powder X-ray (XRD, PAN analytical Empyrean X-ray diffractometer equipped with Cu-Kα radiation source λ= 1.54178Å at 45 kV/ 40 mA); (ii) surface area (SBET) was estimated by the BET (Brunauer-Emmett-Teller) method, pore size and pore volume were determined by the BJH (Barrett-Joyner-Halenda) model. The specific surface area and pore structure characterization were determined by nitrogen adsorption at 77 K using a surface area analyzer Micromeritics Gemini V-2380. The samples were degassed overnight at 373 K before measurement; (iii) surface morphology and quantitative analysis of elemental composition, by surface scanning electron microscopy (SEM) and energy dispersive X-ray spectroscopy (EDX), using a HR-FESEM Hitashi SU-70 operated at 15 kV, equipped with a Bruker Quantax 400 EDS system; (iv) surface functional species by Fourier transform

122 infrared (FTIR, Agilent CARY 630 with wave number range from 400 to 4000 cm^{-1}); (v)
123 basic and acid strength by using Hammett indicators (for basic strength: neutral red, pKa =
124 6.8; bromothymol blue, pKa = 7.2; phenolphthalein, pKa = 9.3; indigo carmine, pKa =
125 12.2; and 2,4-dinitroaniline, pKa = 15.0; indicators for acid strength: bromothymol blue,
126 pKa = 7.2; neutral red, pKa = 6.8; bromocresol purple, pKa = 6.1; bromocresol green, pKa
127 = 4.7; and bromophenol blue, pKa = 3.8). The latter method was carried out by dispersing
128 about 25 mg of the sample (catalyst) in 5.0 mL of a solution of Hammett indicators (0.5 mg
129 of indicator in 10 mL of methanol for basic strength or 10 mL of benzene for acid strength),
130 and left for 2 h to reach the chemical equilibrium. Then, the color of the resulting solution
131 was identified.

132 2.4 FAME synthesis and quantification

133 The experiments for FAME production were carried out in a batch reactor (in glass, 0.25 L
134 of capacity, equipped with temperature control and magnetic agitator), using 2 hours of
135 reaction time at 600 rpm stirring speed.

136 At the end of each batch essay, the catalyst and methanol were separated from the reaction
137 mixture by centrifugation and evaporation, respectively. Then, the supernatant was placed
138 into a separating funnel over 12 h for phase separation. The water contained in the upper
139 layer of the liquid mixture was removed with anhydrous sodium sulfate and weighed. The
140 resulting mixture, hereafter is so-called purified final mixture, was analyzed by gas
141 chromatography for FAME determination and was titrated with a KOH solution for final
142 acid value quantification [14].

143 The Shimadzu G-C 2014 chromatograph used for FAME determination was equipped with
144 a flame ionization detector and a capillary column SGEBP-20 60 m x 0.25 mm i.d. x 0.25
145 µm film thickness with a stationary phase of polyethylene glycol; the carrier gas was
146 helium with a flow rate of 16.7 mL/min and a pressure of 36.1 psi; the injector (AOC-20i)
147 was operated at 200 ºC and an injection volume of 2.0 µL in Split mode. Methyl
148 heptadecanoate was used as internal standard and hexane the solvent. The content of methyl
149 esters was calculated based on the standard method (UNE-EN ISO 14103) [20] and
150 expressed as concentration of FAME using the Eq. 3:

$$C = \frac{\sum A - A_{EI}}{A_{EI}} \times \frac{W_{EI}}{W} \quad (3)$$

151

152 Where C is the concentration of FAME in the purified final mixture (w/w), $\sum A$ is the
153 total peak areas of the methyl ester from C_{14} until $C_{24:1}$, A_{EI} is the peak area corresponding
154 to methyl heptadecanoate, W_{EI} is the mass (mg) of methyl heptadecanoate used and W is
155 the mass (mg) of the sample used in the analysis.

156 The catalyst performance was assessed by the FAME yield and FFA conversion, calculated
157 by Eq. 4 and Eq. 5, respectively [21,22].

$$\text{FAME yield (\%)} = \frac{C \times \text{Total mass of purified final mixture}}{\text{Mass of oil used in the experiment}} \times 100 \quad (4)$$

158

$$\text{FFA conversion (\%)} = \left(1 - \frac{AV_f}{AV_i}\right) \times 100 \quad (5)$$

159

160 Where AV_i and AV_f correspond to the acid value of the initial oil mixture and of the
161 purified final mixture, respectively.

162 2.5 Experimental design and optimization of FAME production process

163 Response Surface Methodology (RSM) based on a Box–Behnken experimental design are a
164 set of mathematical and statistical techniques employed for designing experiments, creating
165 correlations, evaluating the effects of several factors, and their interaction effects for
166 desirable responses. This method uses the minimum required data that give the best
167 reaction condition for a desired response [1,23] and was applied to optimize and to
168 investigate the relationship between operating conditions and the FAME yield. The effect
169 of four independent variables - catalyst loading, methanol/oil, RPO/WCO and reaction
170 temperature on the FAME yield was studied. The experimental range for each independent
171 variable (*aka* factor) tested in this work is shown in Table 1.

172 **Table 1:** Ranges and factor levels of operating variables used in the Box – Behnken
173 experimental design.

Real variables	**Coded variables**	**Level**		
		Low (-1)	Medium (0)	High (+1)
Catalyst loading (wt%)	**A**	5	10	15
Methanol/oil (molar ratio)	**B**	3	6	9
Temperature (^{o}C)	**C**	45	50	55
RPO/WCO (wt%)	**D**	0 (M3)	50 (M2)	100 (M1)

174

175 Twenty nine experimental runs were required, including five replicates of the central point.
176 The correlation in the form of a quadratic polynomial equation was developed for

177 predicting the response (i.e., FAME yield) as a function of independent variables and their
178 interactions according to Eq. 6:

179 $$Y = \beta_0 + \sum_{i=1}^{k} \beta_i x_i + \sum_{i=1}^{k} \beta_{ii} x_i^2 + \sum_{i=1}^{k} \sum_{j=i+1}^{k} \beta_{ij} x_i x_j + \varepsilon \qquad (6)$$

180 Where Y is the predicted response for the process, i.e., the dependent variable; βo is the
181 intercept coefficient (offset); βi are the linear terms; βii are the quadratic terms; βij are the
182 interaction terms; x_i and x_j are the independent variables; and ε is the error [24].

183 Simplified regression models of Eq. 6 (e.g., without interaction terms) were also fitted to
184 the experimental results. The best fit achieved with the simplest model was the one selected
185 and presented in this work.

186 The inference on the regression model was performed through an analysis of variance
187 (ANOVA), for a 95% confidence level, where the statistically significant factors in the
188 response variable were identified, and an analysis of the coefficients of determination of the
189 model, R^2 and adjusted R^2 ("Adj R^2), was used to evaluate the adequacy of the regression
190 model to the experimental data. In this step one used the sum of the squares of residuals,
191 instead of the pure error.

192 Validation of the regression model assumptions (i.e., the assessment of the adequacy of the
193 model) was performed through a residual analysis (normality and residual plots). This
194 analysis was based on normalized/studentized residuals.

195 Once the best regression model was selected and validated, the optimal operating
196 conditions were identified through the response surface. Then, for statistical validity
197 purposes, three runs were performed using those optimal conditions, thus allowing to

198 determine the deviations of the data predicted by the model and the real values obtained
199 experimentally.

200 The software Design – Expert 7.0.0 was used on this statistical data processing and
201 analysis.

202 2.6 Catalyst reusability

203 Recovery, stability and reuse are important aspects of a heterogeneous catalyst to be
204 applied in biodiesel production. The reusability of BFA catalyst in esterification and
205 transesterification reactions was investigated through 2 successive catalytic cycles (i.e., in
206 total 3 cycles) using the optimal reaction conditions found in the optimization step. After
207 each cycle, the solid catalyst was recovered and activated by simple centrifugation, washing
208 with isopropyl alcohol for removing organic compounds eventually retained in the solid
209 surface, calcined at 700 ^{o}C for 3 hours and reused in the next catalytic cycle. At the end of
210 each cycle, the catalyst was characterized by XRD, textural properties and Hammett
211 indicator.

212 3 Results and discussion

213 3.1 Oil mixtures characterization

214 The properties of the oil mixtures prepared for this study are shown in Table 2.

215 **Table 2:** Properties of the oil mixtures used in this work.

	M1	M2	M3

%WCO	0	50	100
%RPO	100	50	0
Moisture (wt%)	0.067±0.010	0.170±0.003	0.197±0.012
Density (g/mL)	0.908±0.008	0.913±0.010	0.906±0.003
AV (mg KOH/g)	0.307±0.004	3.958±0.082	4.934±0.252
FFA (wt%)	0.172±0.005	1.979±0.041	2.453±0.056
MW (g/mol)	843.152±9.522	886.338±1.208	857.825±4.014
Viscosity (mm^2/s)	14.902±0.193	17.122±0.123	19.185±0.392

The properties of M1 (i.e., 100% RPO) are similar to those reported by Kansedo et al. [25] and by Metawea et al. [26]. Concerning the waste cooking oils properties, they are quite dependent of the vegetable oil feedstocks and their frying practices and conditions. The WCO (M3) used in this work has properties similar to those reported by Wan et al. [27] and Lam and Lee [28], and it can be categorized as yellow grease (FFA <15%)[29].

As the percentage of WCO increases in the blend (see Table 2) higher are the moisture and the FFA contents, the acid value and the viscosity, while the remaining properties values (density and molecular weight) are similar among the three blends.

3.2 Catalyst characterization

The solid catalyst prepared was characterized for some textural properties such as specific surface area, crystalline structure, surface functional groups, but also their basic and acid strength, etc. The results are shown and discussed in the next sections.

3.2.1 BET surface area and Hammett indicators analyses

BFA used in this work has an intermediate basic strength (10.1≤ pKb <12.2), due to the high basicity of the metal-oxygen groups (Lewis bases) present in the calcium compounds

on its surface (see Sections 3.2.2 and 3.2.3) and a low acid strength (6.8≤ pKa<7.2) [30]. With regard to its textural properties, BFA has a low (BET) surface area (9.028 m^2/g), characteristic of this type of material, a pore volume of 0.01055 cm^3/g, and an average pore diameter (77.188 Å), which shows some potential to the adsorption and desorption of molecules such as triglycerides, glycerin and FAME [9,31].

The average pore size distribution could be estimated from the nitrogen adsorption-desorption isotherms. Figure 1 shows those isotherms for BFA catalyst, which behaves like a type IV(a) according to the classification of the International Union of Pure and Applied Chemistry. The initial part of this graph exhibits a behavior such as the type II isotherm, typical of monolayer adsorption. Subsequently, a hysteresis cycle associated with the characteristic capillary condensation of mesoporous solids is observed, which is observed for pore size ranges between 20-500 Å [32].

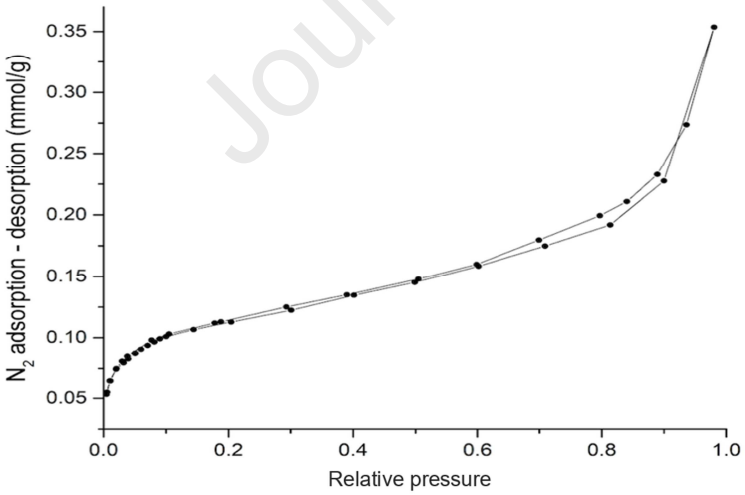

Figure 1: Adsorption and desorption isotherms for the BFA catalyst.

3.2.2 SEM and EDX analysis

The SEM images for characterizing the morphological characteristics and EDX for elemental analysis and chemical characterization of the catalysts were obtained. Figure 2 shows the morphological and the elemental composition of BFA catalyst. Ash particles have uniform distribution of agglomerates with irregular shapes and rough structure. The same characteristics were observed by Rajamma et al. [33]. In addition, the average particle size for the BFA catalyst was 4.353 μm (± 1.07) as determined using the ImageJ software. The results of EDX show as predominant elements: Ca, Mg, Si, Al, O, K, S, Na, Cl and P (Figure 2c).

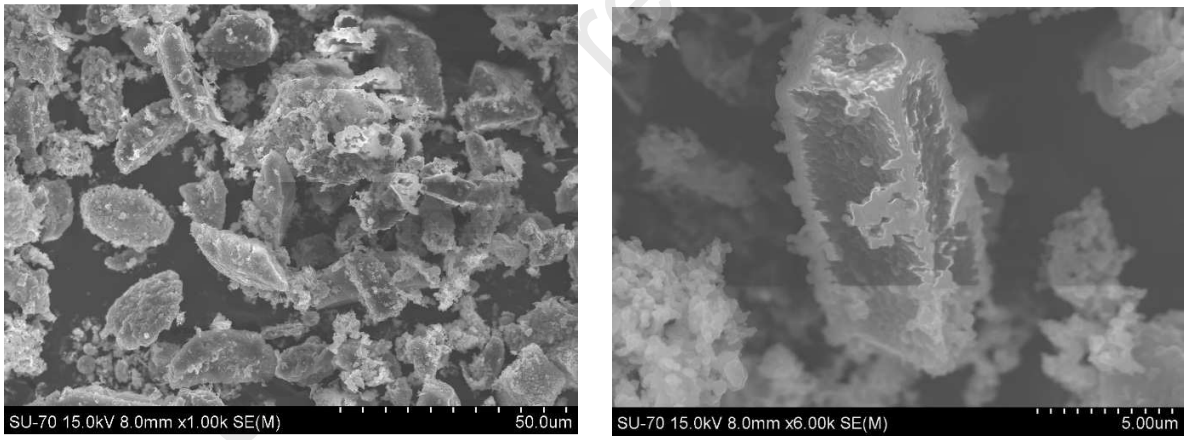

(a) **(b)**

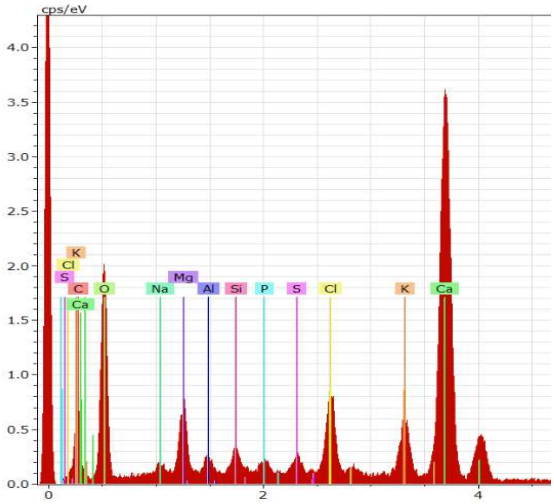

(c)

Figure 2: BFA catalyst characterization by: SEM (a and b) and EDX (c).

3.2.3 XRD analysis

The XRD diffractogram of the BFA catalyst is depicted in Figure 3. The XRD pattern shows clear diffraction peaks corresponding to calcium oxide (CaO) phase detected at 2θ=32.2°, 37.4°, 53.8°, 65.2°, and 67.5°, calcium carbonate ($CaCO_3$-major component) phase detected at 2θ=23.3°, 29.6°, 36.2°, 39.7°, 43.4°, 47.8°, 48.8°, 56.9°, 61.0° and 65.0, potassium chloride (KCl) phase detected at 2θ=28.5°, 40.5°, and silicon dioxide (SiO_2) phase detected at 2θ=20.9°, 26.7°, 36.38°, 39.46°, 40.28°, 50.2°, 60.2° and 68.5°, among other components such as calcium hydroxide deteded at 2θ=17.91°, 28.51°, 33.95°, 47.41°, 50.68°, 64.60°.

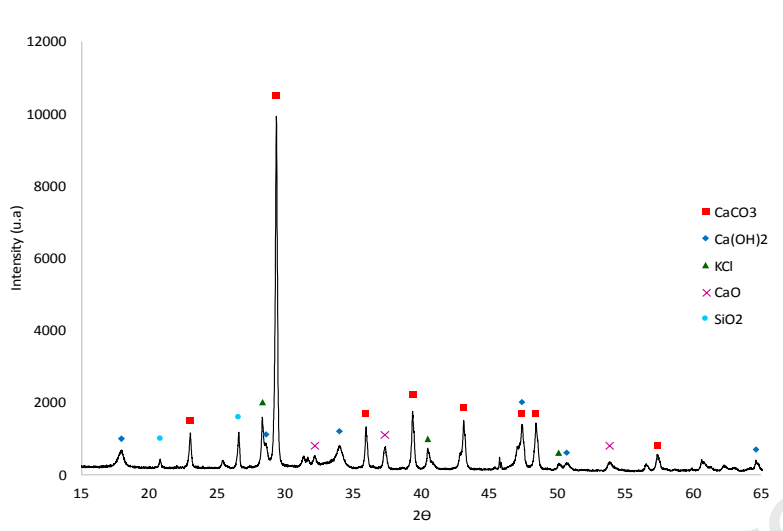

Figure 3: XRD patterns of BFA catalyst

Regarding the semi-quantitative mass composition, a high content of calcium carbonate (71.0 %) was found, followed by calcium hydroxide (12.9 %), potassium chloride (7.1 %), calcium oxide (3.8 %), silicon dioxide (2.3 %) and other components in smaller proportion were identified (3.0 %); similar compounds were reported by Sharma et al. [34] for wood ash and by Ho et al. [35] for palm oil mill fly ash. The presence of calcium hydroxide may be due to the ambient humidity that reacts (after the combustion process) with calcium oxides presents on the surface of the solid; this phenomenon was also observed by Maneerung et al. [30]. The high calcium carbonate content results from the carbonation of calcium oxides and hydroxides since solid material was in contact with atmospheric carbon dioxide, after the combustion process.

3.2.4 FTIR analysis

The FTIR spectrum of BFA used in this work is shown in Figure 4. It shows the major absorption broad band at 1408.1 cm^{-1} and minor absorption bands at 872 and 712 cm^{-1},

280 which correspond to the asymmetric stretching and to out-of-plane band and in-plane band
281 vibration modes of carbonate (CO_3^{2-}) group, respectively. The small bands at 2510 and
282 2320 cm^{-1} also correspond to the characteristic spectrum of this functional group. This
283 result confirms the presence of $CaCO_3$ in BFA, detected by XRD.

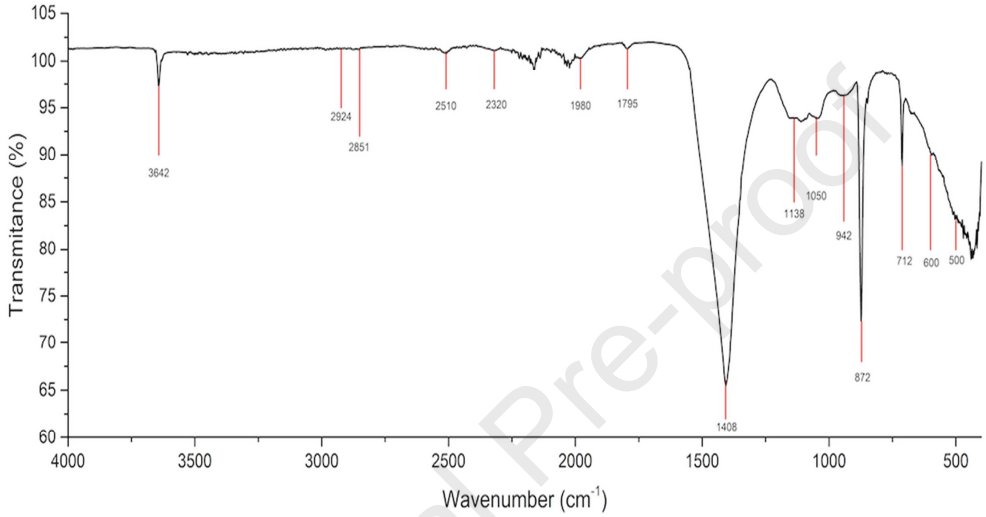

284 **Figure 4:** FTIR spectrum of BFA catalyst.
285

286 PO_4^{-3} and Si-O components (silica phosphates) show broad bands in the region between
287 1138 and 942 cm^{-1}; the same was observed by Maneerung et al. [30] and Sharma et al. [34]
288 in bottom ash waste from woody biomass gasification and wood ash from the combustion
289 of *Acacia nilotica* (babul), respectively. Moreover, the absorption sharp band at 3642 cm^{-1},
290 which is attributed to -OH band, was observed in the BFA catalyst, this band is agreement
291 with the presence of $Ca(OH)_2$ as determined by XRD, and an evidence of the possible water
292 absorption on the CaO surface producing $Ca(OH)_2$ [36].

3.3 Optimization of FAME production process: regression model and statistical analysis

The experimental results obtained in the set of essays aiming at optimizing the FAME yield are shown in Table 3.

Table 3: Experimental design and predicted results of RSM.

	Real variables				FAME yield (wt%)	
Run	Catalyst loading (wt%)	Methanol/oil (mol/mol)	T (°C)	RPO/WCO (wt%)	Experimental	Predicted*
1	15	6	50	100	11.40	21.35
2	10	6	55	0	60.94	63.48
3	10	3	50	0	41.44	41.84
4	10	6	50	50	62.86	55.95
5	10	9	55	50	64.64	62.18
6	15	6	45	50	25.82	31.83
7	10	3	45	50	12.25	17.16
8	10	3	50	100	0.00	6.68
9	5	9	50	50	38.33	35.43
10	10	6	45	0	25.24	26.45
11	5	6	50	100	8.96	1.57
12	15	6	55	50	65.35	68.86
13	10	6	50	50	70.34	55.95
14	5	6	55	50	47.94	49.07
15	10	6	55	100	27.57	28.32
16	10	6	45	100	7.39	-8.70
17	15	3	50	50	52.83	47.22
18	10	9	45	50	33.25	25.16
19	10	9	50	100	8.57	14.68
20	5	3	50	50	28.34	27.43
21	5	6	45	50	0.00	12.05
22	10	9	50	0	40.32	49.83
23	15	6	50	0	68.20	56.51
24	10	6	50	50	38.63	55.95

25	10	3	55	50	59.65	54.18
26	10	6	50	50	45.84	55.95
27	15	9	50	50	57.38	55.21
28	5	6	50	0	38.70	36.73
29	10	6	50	50	62.08	55.95

*Predicted by Eq. 7

The regression model of Eq. 6 fitted to the experimental results revealed that the interaction between the factors ($\beta_{ij}x_i x_j$) was not significant (p-value > 0.05). Thus, the simplified model (i.e., quadratic model without interactions) was used and the goodness-of-fit was evaluated by the several parameters determined in the ANOVA. The results are shown in Table **4**, where it can be seen that model has a good fit as R^2=0.8702 and Adj R^2=0.8182. The R^2 value indicates that 87.02 % of the variability in the data is predicted by the model.

Table 4: ANOVA results of the response surface quadratic model without interactions.

Source of variations	**Sum of squares**	**Degrees of freedom**	**Mean square**	**F - value**	**p – value**
Model	12028.36	8	1503.55	16.75	< 0.0001
Residual	1794.79	20	89.74		
Lack of fit	1100.2	16	68.76	0.936	0.9183
Pure error	694.59	4	173.65		
Total	13823.15	28			
	R^2 = 0.8702	Adj R^2 = 0.8182	Pred R^2 = 0.7424	C.V.[a] = 24.88%	S.D.[b] = 9.47

[a] C.V.= coefficient of variation.

[d] S.D.= standard deviation.

.

The low p-value (< 0.0001) of the model means that it is statistically significant. On the other hand, the lack of fit F-value of 0.936 implies that is not significant relative to the pure error, i.e. the lack of fit of the model is statistically non-significant; there is a 91.83 % chance that this value could occur due to noise. The "Pred R^2" of 0.7424 is in reasonable

agreement with the "Adj R^2" value of 0.8182. In short, the selected regression model satisfactorily predicts the effect of the four factors on FAME yield. Eq. 7 represents the model developed:

$$Y = 55.95 + 9.89\,x_A + 4.00\,x_B + 18.51\,x_C - 17.58\,x_D - 6.92\,x_A^2 - 7.70\,x_B^2 - 8.57x_C^2 - 19.98x_D^2 \quad (7)$$

Where Y is the response variable (FAME yield, wt%), x_A (catalyst loading, wt%), x_B (methanol/oil, molar ratio), x_C (reaction temperature, ^oC) and x_D (RPO/WCO, wt%) are the studied factors. The positive sign of a coefficient term means synergistic effect while the negative sign reveals the opposite effect, of the influencing variables on FAME yield [1]. The FAME yield predicted by this regression model is shown in Table 3, for comparison with experimental results.

The statistical significance of each regression coefficient of the model on the response variable was evaluated using ANOVA testing and the results are shown in Table 5**:**. The p-values indicate the significance of each regression coefficient. In general, smaller p-value (< 0.05) indicates higher significance of the corresponding coefficient [37]. According to obtained results, three of the four linear factors were statistically significant (x_A, x_C, and x_D) and only one (x_B) was not significant (for confidence level of 95%). Besides that, the influence of square value of RPO/WCO (x_D^2) with a negative effect of -19.98 (p-value < 0.0001) was found to be the most significant term affecting the FAME yield; the quadratic term of the temperature was also significant (p-value = 0.0320).

Table 5: ANOVA results for the coefficients of the variables in the quadratic regression model without interactions.

Model parameters	Estimate coefficient	F - value	p - value
Intercept	55.95		
x_A	9.89	13.09	0.0017
x_B	4.00	2.14	0.1592
x_C	18.51	45.82	< 0.0001
x_D	-17.58	0.158	< 0.0001
x_A^2	-6.92	3.46	0.0775
x_B^2	-7.70	4.29	0.0515
x_C^2	-8.57	5.31	0.0320
x_D^2	-19.98	28.88	< 0.0001

In order to validate the assumptions of the simplified regression model (i.e., quadratic model without interactions), statistical graphical methods were used. A normal probability plot of residuals is shown in Figure 5a, which corresponds to the difference between the experimental and the predicted response. The data points are located approximately along a straight line, thus one can intuitively conclude that the residuals follow a normal distribution. Plot of residuals versus fitted response values (predicted) is depicted in Figure 5b, which shows that the residuals are randomly distributed. Residuals are located in a horizontal line and the number of points that exist in the above and below of horizontal line is equal. Moreover, residual values are in the range ± 3.00; typically, a threshold of three standard deviations is employed as a definition of an outlier [38]. The actual FAME yield versus the predicted values is plotted in Figure 5c, which corroborates the goodness-of-fit of the regression model developed. In brief, this analysis confirms the accuracy and reliability of the proposed regression model.

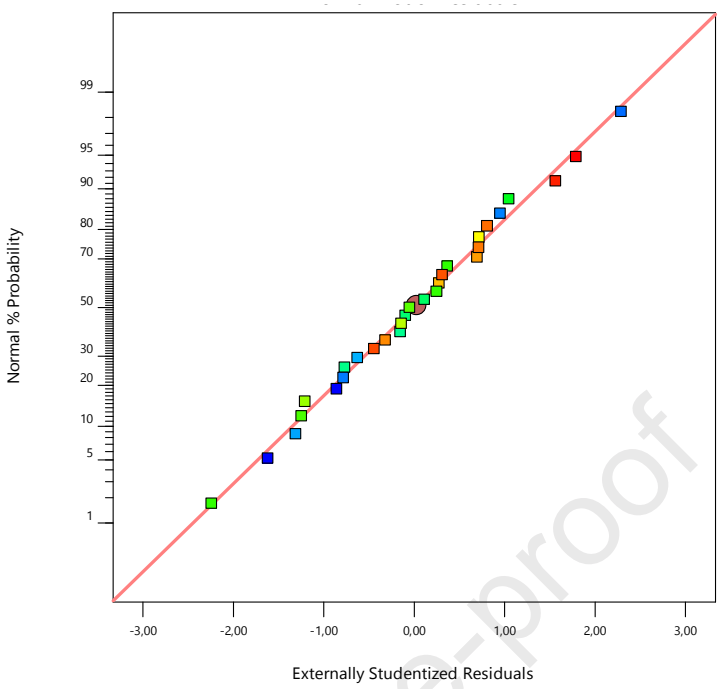

(a)

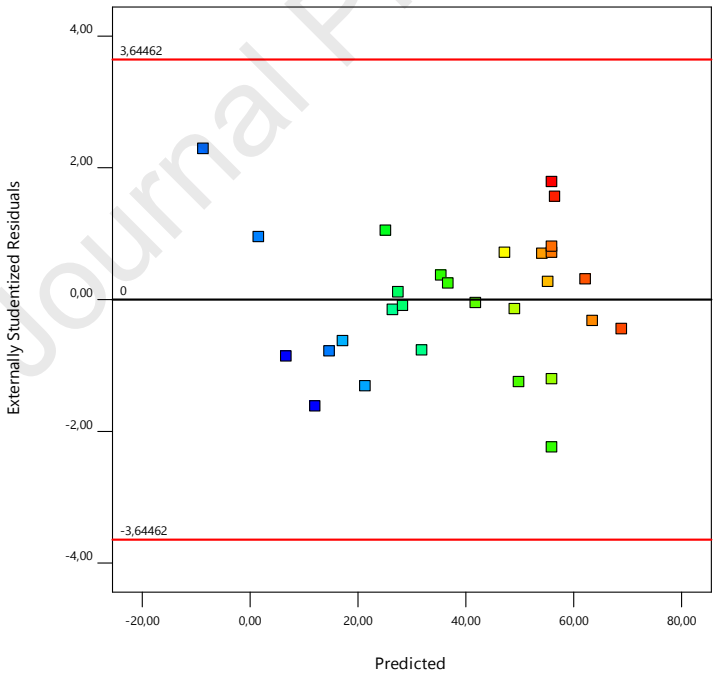

(b)

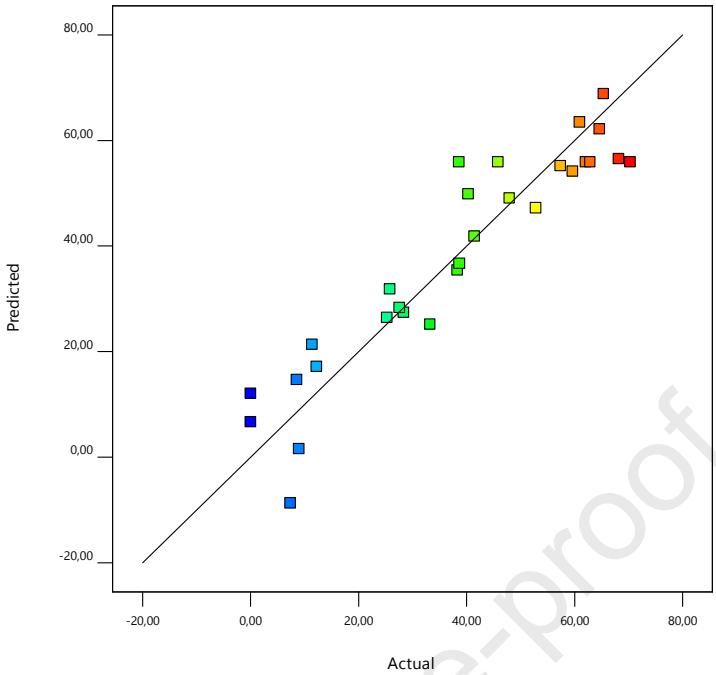

(c)

Figure 5: (a) Residual normal probability plot, (b) Residual versus predicted response plot, (c) Predicted versus actual values plot.

As stated before, in the ranges tested (Table 1), the factors studied in this work, except methanol/oil molar ratio, had a statistically significant influence on FAME yield; although some were more significant than others. This is shown as response surface plots in Figure 6.

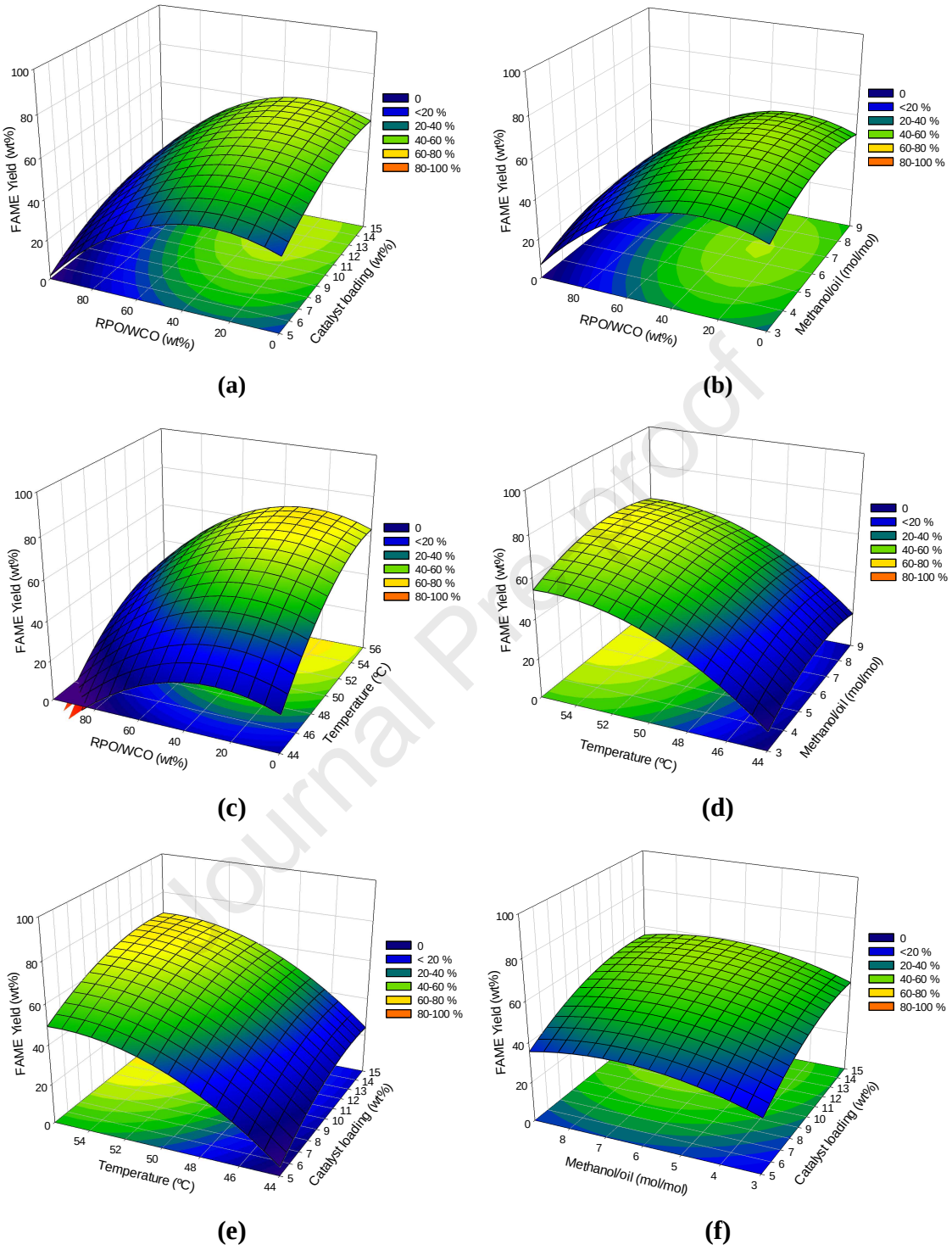

354 **Figure 6:** Response surface plots of FAME yield as a function of: (a) RPO/WCO ratio and
355 catalyst loading at 50 ºC and methanol/oil = 6 mol/mol; (b) RPO/WCO ratio and

356 methanol/oil at 50 ºC and catalyst loading = 10 wt%; (c) RPO/WCO ratio and temperature
357 for catalyst loading = 10 wt% and methanol/oil = 6 mol/mol; (d) temperature and
358 methanol/oil ratio for catalyst loading = 10 wt% and RPO/WCO = 50 wt%; (e) temperature
359 (^{o}C) and catalyst loading (wt%) for methanol/oil = 6 mol/mol and RPO/WCO = 50 wt%; (f)
360 methanol/oil ratio and catalyst loading (wt%) at 50 ºC and RPO/WCO = 50 wt%.

361

362 From Figure 6a, higher yields of FAME (64 %) were achieved with high catalyst loading
363 (13.2 wt%) and moderate (28.0 wt%) RPO/WCO mass ratio. For any fixed RPO/WCO
364 mass ratio, as catalyst loading increased higher FAME yields were observed, which may be
365 due to the higher number of active sites (of the catalyst) available in the reaction medium.
366 On the other hand, RPO/WCO mass ratio higher that 28.0 wt% affected negatively the
367 FAME yield for any catalyst loading tested. Thus, the low acid strength and intermediate
368 basic strength of BFA seems to be suitable to catalyze oily mixtures with higher FFA
369 contents, which, according to some authors [21,39], could be due to the balance of acid and
370 basic catalyst sites. This is a promising result for the economic and environmental
371 sustainability of the process. Concerning methanol/oil molar ratio, Figure 6b shows the
372 weak influence of this factor on the response variable; therefore, the methanol/oil molar
373 ratio of 6.6 can be used to achieve the highest yields to FAME (64 %). Similar behavior
374 was mentioned by Volli et al. [40] for the same methanol/oil molar ratio but using bone
375 impregnated fly ash as a catalyst. Figure 6c shows the influence on FAME yield of the two
376 most significant factors studied in this work: temperature and RPO/WCO mass ratio.
377 Indeed, increasing the reaction temperature rose the FAME yield independently of the

RPO/WCO mass ratio used. The higher yield was observed at 55 ^{o}C with 28.0 wt% of RPO/WCO mass ratio (loading = 10 wt% and methanol/oil = 6 mol/mol); Uprety et al. [22] also found a very significant effect between 50 and 60 ^{o}C (reaction temperature) on the yield, using a catalyst of CaO and RPO as raw material. Figure 6d shows once more the different relevance of the temperature and methanol/oil molar ratio on the response variable. Catalyst loading and reaction temperature had similar positive effects on the FAME yield (Figure 6e), being the higher yields achieved (c.a. 74 %) at 55 ^{o}C and catalyst loading 13.2 wt% (for methanol/oil molar ratio of 6 and RPO/WCO mass ratio of 50 wt%). This high FAME yield achieved may be due to the crystalline phases (calcium hydroxide and calcium oxide), the functional groups (carbonate group) and pore diameter (average 77.188 Å) found in the solid catalyst.

Regarding the percentage of conversion of free fatty acids, similar results were obtained for the different experiments with values close to 84.3 % ± 6.0 %; which may be due to the slightly acid character of the solid catalyst (6.8≤ pKa<7.2). These conversion values point out to a bifunctional character of the BFA catalyst, i.e., simultaneous catalysis of transesterification and esterification reactions, already found by Vargas et al. [13].

Optimal operating condition

An important objective of this study was to find optimal operating conditions to achieve maximum FAME yield, combining the several independent variables studied. The RMS suggested that the highest FAME yield was 73.8 %, which can be achieved by using 13.57 wt% of catalyst loading, 6.7 methanol/oil molar ratio, 28.04 wt% of RPO/WCO mass ratio and 55 ^{o}C for the reaction temperature. To validate the proposed operating conditions, three

replicate experiments were conducted under them, over 2 hours at 600 rpm stirring speed. The average experimental FAME yield was 78.8 % (± 1.7 %), which is close to the predicted value (i.e., 73.8 %). So, the validity of the proposed correlation is confirmed again with an error of 6.8 % (±0.05%). The FAME yield and the respective relative error between model predictions and experimental value were close to the obtained by Badday et al. [41], using activated carbon-supported tungstophosphoric as catalyst on the Jatropha oil and a Central Composite Design (CCD) as experimental design method.

3.4 Catalyst reusability: catalytic performance assessment

The reusability of a catalyst is very important for its commercial feasibility. In order to investigate the reusability of the BFA catalyst, the subsequent reaction cycles were carried out under the optimized reaction condition: 13.57 wt% of catalyst loading, 6.7 methanol/oil molar ratio, 28.04 wt% of RPO in the oil mixture and 55 ^{o}C for the reaction temperature, 2 h reaction time and 600 rpm stirring speed. Between each cycle the catalyst was regenerated, according to the procedure stated in Section 2.6. The FAME yields obtained from the reused catalyst in each cycle is shown in Figure 7, where a slight increase on FAME yield with the repeated usage of the catalyst is observed. However, a statistical analysis of the data (ANOVA for a confidence level of 95%) showed that differences observed among the three essays were not statistically significant with p-value = 0.1258; therefore, the activity of the BFA catalyst could be considered roughly constant over three cycles of use. Similar catalytic stability were reported by Chakraborty et al. [9] and

420 Maneerung et al. [30] using fly ash from a thermal power plant with a combustion
421 technology and bottom ash waste arising from woody biomass gasification, respectively.

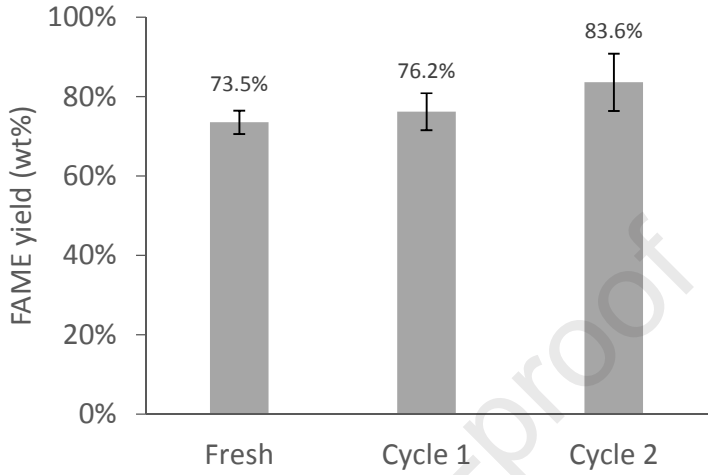

422

423 **Figure 7:** Reusability studies of the BFA catalyst under the optimal operating conditions.

424 The XRD patterns of the reused catalyst after each regeneration cycle are shown in Figure
425 8. It can be observed in the superimposed diffractograms that the majority phase was
426 calcium carbonate ($CaCO_3$), phase detected at $2\theta=23.3^o$, 29.6^o, 36.2^o, 39.7^o, 43.4^o, 47.8^o,
427 48.8^o and 56.9^o, followed by calcium hydroxide ($Ca(OH)_2$) deteded at $2\theta=17.91°$, 33.95°
428 and 50.68°, indicating that CaO was partially transformed into $Ca(OH)_2$, probably through
429 the reaction of CaO ($2\theta=32.2°$, 37.4° and 53.8°) with H_2O in small amount in the reactants
430 and/or moisture during the repeated usage of catalyst [30]. This may explain the observed
431 slight increase of FAME yield over the reuse cycles of the BFA, as $Ca(OH)_2$ has catalytic
432 properties. A peak is also observed in $2\theta= 26.7^o$ due to the presence of the phase silicon
433 dioxide (SiO_2) that gives the catalyst a low acid strength (and thus a bifunctional). The KCl
434 ($2\theta=28.5^o$ and 40.5^o) found did not contribute to the catalytic activity of the BFA. This

435 conclusion arose from three experimental tests performed with pure KCl as a catalyst and
436 where no FAME yield was registered (results not shown).

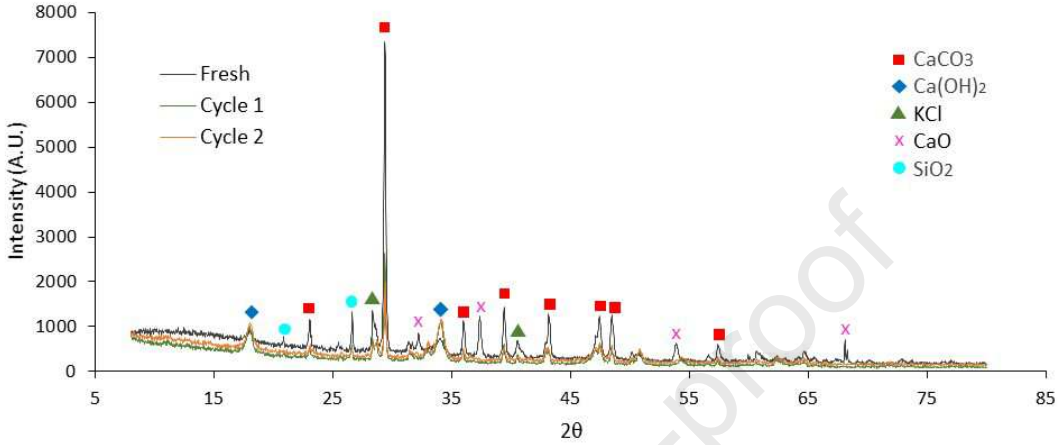

437

438 **Figure 8:** XRD patterns of BFA catalyst for the different reuse cycles.
439

440 The BET surface area, pore volume, pore diameter and basic and acid strength of reused
441 catalyst (BFA) are shown in Table 6. The basic and acid strength of this reused catalyst and
442 its textural properties did not change throughout the reuse cycles and regeneration steps.

443 **Table 6:** Textural properties and acid/basic strength of the BFA catalyst used in three
444 FAME synthesis cycles.

Catalyst sample	Specific surface area (m^2/g)	Pore volume (cm^3/g)	Average pore diameter (Å)	Basic strength	Acid strength
Fresh	9.0280	0.01055	77.188	10.1≤ pKa <12.2	6.8≤ pKa<7.2
Cycle 1	10.9496	0.01253	82.639	10.1≤ pKa <12.2	6.8≤ pKa<7.2
Cycle 2	10.2876	0.01147	80.365	10.1≤ pKa <12.2	6.8≤ pKa<7.2

445

From these results, it is reasonable to conclude that after the cycles of reuse of the catalyst, it did not lose its catalytic activity (FAME yield). Indeed, the catalytic activity seems to be slightly increased, although not statistically different between the tests done, which can be explained due to relatively small changes of its textural properties, crystalline active phases ($CaCO_3$, $Ca(OH)_2$ and SiO_2) and basic and acid strength (surface chemistry) throughout the reuse cycles. Thus, BFA catalyst has shown good properties of reuse in the process, and that is an advantage, because it is a low cost material, produced from an industrial waste and thus can turn the process more sustainable in terms of natural resources integration.

4 Conclusions

An efficient fly ash residual catalyst (BFA) was evaluated with mixtures of RPO and WCO to produce FAME using the response surface methodology and an experimental design Box Behnken type for optimizing the response variable (FAME yield). A regression quadratic model without interactions was the one that best fitted the experimental results, predicting the following optimal operating conditions: batch regime over 2 h and 600 rpm of stirring speed, catalyst loading of 13.57 wt%, methanol/oil molar ratio of 6.7, RPO in the oil mixture of 28.04 wt%, temperature of 55 ^{o}C. Under these operating conditions maximum FAME yield expected is 73.8 %. In the tested ranges, the most significant variables (95 % confidence level) affecting the FAME yield were the RPO/WCO mass ratio and the reaction temperature (^{o}C), both with p-value <0.0001, followed by the catalyst loading (p-value = 0.0017). On the other hand, the methanol/oil molar ratio was not significant (p-

466 value = 0.1592), indicating that the lowest ratio tested can be used to achieve the higher
467 FAME yield registered.

468 The selected regression model accurately predicted the experimental results with a R^2 =
469 0.8702 and Adj R^2 = 0.8182. Three essays were carried out under the optimal operating
470 conditions, where the average of FAME yield reached was 78.8% (± 1.7 %), near the
471 predicted by the regression model (73.8 %). Thus, the validity of the proposed regression
472 model was demonstrated.

473 This works showed that BFA catalyst can be used for up to three cycles without loss of
474 catalytic activity. However, the catalyst should be regenerated between each cycle, by
475 washing with isopropyl alcohol and calcined at 700 ^{o}C for 3 h. The characterization of the
476 surface, textural and crystalline properties of the catalyst, after use in each FAME synthesis
477 cycle, showed that those properties were not significantly affected. The acid and basic
478 strength remained constants. In addition, one recommends to evaluate the reuse of BFA
479 above three cycles in order to find the maximum number of cycles that it could be used
480 keeping a high FAME yield and carry out a complementary characterization of the acid and
481 basic catalyst sites with temperature-programmed desorption of NH_3 and CO_2 techniques,
482 respectively.

483 Summing up, exploiting residual feedstocks, this work gives a sustainable and affordable
484 approach to lower the biodiesel production costs and simultaneously, minimizing the
485 environmental burdens traditionally inherent to the management of two wastes streams:
486 WCO and BFA.

Therefore, an awareness should be created so that any material that is deemed a waste could be exploited for usage in this or other applications, thereby implementing the principles of circular economy.

Acknowledgments

Edgar M. Vargas S. expresses his sincere gratitude to the Universidad Jorge Tadeo Lozano (Direction of Investigation, Creation and Extension) for the financial assistance of this work. Márcia C. Neves acknowledges FCT, I.P. for the research contract CEECIND/00383/2017 under the CEEC Individual 2017. The authors thank for the financial support to FCT/MCTES for the financial support to CESAM (UIDP/50017/2020 & UIDB/50017/2020) and CICECO (UIDB/50011/2020 & UIDP/50011/2020) through national funds.

References

[1] W. Liu, P. Yin, X. Liu, R. Qu, Design of an effective bifunctional catalyst organotriphosphonic acid-functionalized ferric alginate (ATMP-FA) and optimization by Box-Behnken model for biodiesel esterification synthesis of oleic acid over ATMP-FA, Bioresour. Technol. 173 (2014) 266–271. https://doi.org/10.1016/j.biortech.2014.09.087.

[2] D.Y.C. Leung, X. Wu, M.K.H. Leung, A review on biodiesel production using catalyzed transesterification, Appl. Energy. 87 (2010) 1083–1095.

https://doi.org/10.1016/j.apenergy.2009.10.006.

[3] N. Mansir, S.H. Teo, U. Rashid, M.I. Saiman, Y.P. Tan, G.A. Alsultan, Y.H. Taufiq-Yap, Modified waste egg shell derived bifunctional catalyst for biodiesel production from high FFA waste cooking oil. A review, Renew. Sustain. Energy Rev. 82 (2018) 3645–3655. https://doi.org/10.1016/j.rser.2017.10.098.

[4] I. Nurfitri, G.P. Maniam, N. Hindryawati, M.M. Yusoff, S. Ganesan, Potential of feedstock and catalysts from waste in biodiesel preparation: A review, Energy Convers. Manag. 74 (2013) 395–402. https://doi.org/10.1016/j.enconman.2013.04.042.

[5] A. Demirbas, Biodiesel from waste cooking oil via base-catalytic and supercritical methanol transesterification, Energy Convers. Manag. 50 (2009) 923–927. https://doi.org/10.1016/j.enconman.2008.12.023.

[6] J.W. Chen, S.L. Wang, D.P.H. Hsieh, H.H. Yang, H.L. Lee, Carcinogenic potencies of polycyclic aromatic hydrocarbons for back-door neighbors of restaurants with cooking emissions, Sci. Total Environ. 417–418 (2012) 68–75. https://doi.org/10.1016/j.scitotenv.2011.12.012.

[7] P.L. Boey, G.P. Maniam, S.A. Hamid, Biodiesel production via transesterification of palm olein using waste mud crab (Scylla serrata) shell as a heterogeneous catalyst, Bioresour. Technol. 100 (2009) 6362–6368. https://doi.org/10.1016/j.biortech.2009.07.036.

[8] I.M. Mendonça, O.A.R.L. Paes, P.J.S. Maia, M.P. Souza, R.A. Almeida, C.C. Silva,

S. Duvoisin, F.A. de Freitas, New heterogeneous catalyst for biodiesel production from waste tucumã peels (Astrocaryum aculeatum Meyer): Parameters optimization study, Renew. Energy. 130 (2019) 103–110. https://doi.org/10.1016/j.renene.2018.06.059.

[9] R. Chakraborty, S. Bepari, A. Banerjee, Transesterification of soybean oil catalyzed by fly ash and egg shell derived solid catalysts, Chem. Eng. J. 165 (2010) 798–805. https://doi.org/10.1016/j.cej.2010.10.019.

[10] M.S. Kotwal, P.S. Niphadkar, S.S. Deshpande, V. V. Bokade, P.N. Joshi, Transesterification of sunflower oil catalyzed by flyash-based solid catalysts, Fuel. 88 (2009) 1773–1778. https://doi.org/10.1016/j.fuel.2009.04.004.

[11] R.P. Girón, R.R. Gil, I. Suárez-Ruiz, E. Fuente, B. Ruiz, Adsorbents/catalysts from forest biomass fly ash. Influence of alkaline activating agent, Microporous Mesoporous Mater. 209 (2015) 45–53. https://doi.org/10.1016/j.micromeso.2015.01.051.

[12] A. Chatterjee, X. Hu, F.L.Y. Lam, Catalytic activity of an economically sustainable fly-ash-metal-organic- framework composite towards biomass valorization, Catal. Today. 314 (2018) 137–146. https://doi.org/10.1016/j.cattod.2018.01.018.

[13] E.M. Vargas, M.C. Neves, L.A.C. Tarelho, M.I. Nunes, Solid catalysts obtained from wastes for FAME production using mixtures of refined palm oil and waste cooking oils, Renew. Energy. 136 (2019) 873–883. https://doi.org/10.1016/j.renene.2019.01.048.

548 [14] ICONTEC, NTC 218. Grasas y aceites vegetales y animales. Determinación del
549 índice de acidez y de la acidez., Colombia, 2011. https://tienda.icontec.org/wp-
550 content/uploads/pdfs/NTC218.pdf (accessed February 15, 2019).

551 [15] ICONTEC, Grasas y aceites animales y vegetales. Método de la determinación de la
552 densidad (masa por volumen convencional). NTC 336., 2016.

553 [16] ICONTEC, Grasas y aceites animales y vegetales. Determinación del índice de
554 saponificación. NTC 335., 1998.

555 [17] ASTM, Standard Specifications and Operating Instructions for Glass Capillary
556 Kinematic Viscometers. ASTM D446 - 12, 2017.
557 https://www.astm.org/Standards/D446.htm (accessed February 15, 2019).

558 [18] S. Specifications, ASTM standard D446–07, Standard Specifications and Operating
559 Instructions for Glass Capillary Kinematic Viscometers, ASTM Int. 100 Barr Harb.
560 Drive, PO Box C700, West Conshohocken, PA 19428-2959, United States. (2009)
561 1–24. https://doi.org/10.1520/D0446-07.2.

562 [19] G. Leofanti, G. Tozzola, M. Padovan, G. Petrini, S. Bordiga, A. Zecchina, Catalyst
563 characterization: characterization techniques, 1997. https://ac-els-cdn-
564 com.ezproxy.unal.edu.co/S0920586196000569/1-s2.0-S0920586196000569-
565 main.pdf?_tid=19d5e4b8-7ff0-4112-8d38-
566 dcc4bfd030cd&acdnat=1550332601_264d3d96907b4cb6bcc5cdfbeff93007
567 (accessed February 16, 2019).

568 [20] AENOR-EN 14103, Productos derivados de aceites y grasas. Ésteres metílicos de

ácidos grasos (FAME). Determinación de los contenidos de éster y de éster metílico del ácido linolénico., España, 2011. www.agilent.com/chem. (accessed February 15, 2019).

[21] W.N.N. Wan Omar, N.A.S. Amin, Biodiesel production from waste cooking oil over alkaline modified zirconia catalyst, Fuel Process. Technol. 92 (2011) 2397–2405. https://doi.org/10.1016/j.fuproc.2011.08.009.

[22] B.K. Uprety, W. Chaiwong, C. Ewelike, S.K. Rakshit, Biodiesel production using heterogeneous catalysts including wood ash and the importance of enhancing byproduct glycerol purity, Energy Convers. Manag. 115 (2016) 191–199. https://doi.org/10.1016/j.enconman.2016.02.032.

[23] B. Salamatinia, H. Mootabadi, S. Bhatia, A.Z. Abdullah, Optimization of ultrasonic-assisted heterogeneous biodiesel production from palm oil: A response surface methodology approach, Fuel Process. Technol. 91 (2010) 441–448. https://doi.org/10.1016/j.fuproc.2009.12.002.

[24] Z. Hajamini, M.A. Sobati, S. Shahhosseini, B. Ghobadian, Waste fish oil (WFO) esterification catalyzed by sulfonated activated carbon under ultrasound irradiation, Appl. Therm. Eng. 94 (2016) 1–10. https://doi.org/10.1016/j.applthermaleng.2015.10.101.

[25] J. Kansedo, K.T. Lee, S. Bhatia, Cerbera odollam (sea mango) oil as a promising non-edible feedstock for biodiesel production, Fuel. 88 (2009) 1148–1150. https://doi.org/10.1016/j.fuel.2008.12.004.

590 [26] R. Metawea, T. Zewail, E.S. El-Ashtoukhy, I. El Gheriany, H. Hamad, Process
591 intensification of the transesterification of palm oil to biodiesel in a batch agitated
592 vessel provided with mesh screen extended baffles, Energy. 158 (2018) 111–120.
593 https://doi.org/10.1016/j.energy.2018.06.007.

594 [27] W.N.N. Wan Omar, N.A. Saidina Amin, Optimization of heterogeneous biodiesel
595 production from waste cooking palm oil via response surface methodology, Biomass
596 and Bioenergy. 35 (2011) 1329–1338.
597 https://doi.org/10.1016/j.biombioe.2010.12.049.

598 [28] M.K. Lam, K.T. Lee, Accelerating transesterification reaction with biodiesel as co-
599 solvent: A case study for solid acid sulfated tin oxide catalyst, Fuel. 89 (2010) 3866–
600 3870. https://doi.org/10.1016/j.fuel.2010.07.005.

601 [29] M.R. Avhad, J.M. Marchetti, A review on recent advancement in catalytic materials
602 for biodiesel production, Renew. Sustain. Energy Rev. 50 (2015) 696–718.
603 https://doi.org/10.1016/j.rser.2015.05.038.

604 [30] T. Maneerung, S. Kawi, C.H. Wang, Biomass gasification bottom ash as a source of
605 CaO catalyst for biodiesel production via transesterification of palm oil, Energy
606 Convers. Manag. 92 (2015) 234–243.
607 https://doi.org/10.1016/j.enconman.2014.12.057.

608 [31] K. Jacobson, R. Gopinath, L.C. Meher, A.K. Dalai, Solid acid catalyzed biodiesel
609 production from waste cooking oil, Appl. Catal. B Environ. 85 (2008) 86–91.
610 https://doi.org/10.1016/j.apcatb.2008.07.005.

611 [32] M. Thommes, K. Kaneko, A. V Neimark, J.P. Olivier, F. Rodriguez-Reinoso, J.
612 Rouquerol, K.S.W. Sing, IUPAC Technical Report Physisorption of gases, with
613 special reference to the evaluation of surface area and pore size distribution (IUPAC
614 Technical Report), (2015). https://doi.org/10.1515/pac-2014-1117.

615 [33] R. Rajamma, R.J. Ball, L.A.C. Tarelho, G.C. Allen, J.A. Labrincha, V.M. Ferreira,
616 Characterisation and use of biomass fly ash in cement-based materials, J. Hazard.
617 Mater. 172 (2009) 1049–1060. https://doi.org/10.1016/j.jhazmat.2009.07.109.

618 [34] M. Sharma, A.A. Khan, S.K. Puri, D.K. Tuli, Wood ash as a potential heterogeneous
619 catalyst for biodiesel synthesis, Biomass and Bioenergy. 41 (2012) 94–106.
620 https://doi.org/10.1016/j.biombioe.2012.02.017.

621 [35] W.W.S. Ho, H.K. Ng, S. Gan, S.H. Tan, Evaluation of palm oil mill fly ash
622 supported calcium oxide as a heterogeneous base catalyst in biodiesel synthesis from
623 crude palm oil, Energy Convers. Manag. 88 (2014) 1167–1178.
624 https://doi.org/10.1016/j.enconman.2014.03.061.

625 [36] P.L. Boey, S. Ganesan, S.X. Lim, S.L. Lim, G.P. Maniam, M. Khairuddean,
626 Utilization of BA (boiler ash) as catalyst for transesterification of palm olein,
627 Energy. 36 (2011) 5791–5796. https://doi.org/10.1016/j.energy.2011.09.005.

628 [37] J.M. Avramović, O.S. Stamenković, Z.B. Todorović, M.L. Lazić, V.B. Veljković,
629 The optimization of the ultrasound-assisted base-catalyzed sunflower oil
630 methanolysis by a full factorial design, Fuel Process. Technol. 91 (2010) 1551–1557.
631 https://doi.org/10.1016/j.fuproc.2010.06.001.

[38] I. Noshadi, N.A.S. Amin, R.S. Parnas, Continuous production of biodiesel from waste cooking oil in a reactive distillation column catalyzed by solid heteropolyacid: Optimization using response surface methodology (RSM), Fuel. 94 (2012) 156–164. https://doi.org/10.1016/j.fuel.2011.10.018.

[39] M.F. Rabiah Nizah, Y.H. Taufiq-Yap, U. Rashid, S.H. Teo, Z.A. Shajaratun Nur, A. Islam, Production of biodiesel from non-edible Jatropha curcas oil via transesterification using Bi2O3-La2O3 catalyst, Energy Convers. Manag. 88 (2014) 1257–1262. https://doi.org/10.1016/j.enconman.2014.02.072.

[40] V. Volli, M.K. Purkait, C.M. Shu, Preparation and characterization of animal bone powder impregnated fly ash catalyst for transesterification, Sci. Total Environ. 669 (2019) 314–321. https://doi.org/10.1016/j.scitotenv.2019.03.080.

[41] A.S. Badday, A.Z. Abdullah, K.T. Lee, Optimization of biodiesel production process from Jatropha oil using supported heteropolyacid catalyst and assisted by ultrasonic energy, Renew. Energy. 50 (2013) 427–432. https://doi.org/10.1016/j.renene.2012.07.013.

Highlights

- Waste cooking oil and biomass fly ash were used to produce FAME.
- RSM was used to optimize four operating reaction parameters.
- Catalytic activity of the biomass fly ash was kept over three cycles.
- Valorization of residual feedstocks with a sustainable and affordable approach.

Declaration of interests

☒ The authors declare that they have no known competing financial interests or personal relationships that could have appeared to influence the work reported in this paper.

☐The authors declare the following financial interests/personal relationships which may be considered as potential competing interests: